Published in final edited form as:
Bioconjug Chem. 2012 December 19; 23(12): 2377–2385. doi:10.1021/bc3003919.

Synthesis and Biological Evaluation of Low Molecular Weight Fluorescent Imaging Agents for the Prostate-Specific Membrane Antigen

Ying Chen[†], **Mrudula Pullambhatla**[†], **Sangeeta R. Banerjee**[†], **Youngjoo Byun**[‡], **Marigo Stathis**[§], **Camilo Rojas**[§], **Barbara S. Slusher**[§], **Ronnie C. Mease**[†], and **Martin G. Pomper**[*,†]

[†]Russell H. Morgan Department of Radiology, Brain Science Institute, Johns Hopkins Medical School, Baltimore, Maryland 21231, United States

[§]NeuroTranslational Drug Discovery Program, Brain Science Institute, Johns Hopkins Medical School, Baltimore, Maryland 21231, United States

[‡]College of Pharmacy, Korea University, 2511 Sejong-ro, Jochiwon-eup, Yeongi-gun, Chungnam 339–700, South Korea

Abstract

Targeted near-infrared (NIR) optical imaging can be used in vivo to detect specific tissues, including malignant cells. A series of NIR fluorescent ligands targeting the prostate-specific membrane antigen (PSMA) was synthesized and each compound was tested for its ability to image PSMA+ tissues in experimental models of prostate cancer. The agents were prepared by conjugating commercially available active esters of NIR dyes, including IRDye800CW, IRDye800RS, Cy5.5, Cy7, or a derivative of indocyanine green (ICG) to the terminal amine group of (*S*)-2-(3-((*S*)-5-amino-1-carboxypentyl)ureido)pentanedioic acid **1**, (14S,18*S*)-1-amino-8,16-dioxo-3,6-dioxa-9,15,17-triazaicosane-14,18,20-tricarboxylic acid **2** and (3*S*,7*S*)-26-amino-5,13,20-trioxo-4,6,12,21-tetraaza-hexacosane-1,3,7,22-tetracarboxylic acid **3**. The $\mathbf{K}_i$ values for the dye-inhibitor conjugates ranged from 1 to 700 pM. All compounds proved capable of imaging PSMA+ tumors selectively to varying degrees depending on the choice of fluorophore and linker. The highest tumor uptake was observed with IRDye800CW employing a poly(ethylene glycol) or lysine-suberate linker, as in 800CW-**2** and 800CW-**3**, while the highest tumor to nontarget tissue ratios were obtained for Cy7 with these same linkers, as in Cy7-**2** and Cy7-**3**. Compounds **2** and **3** provide useful scaffolds for targeting of PSMA+ tissues in vivo and should be useful for preparing NIR dye conjugates designed specifically for clinical intraoperative optical imaging devices.

[*]**Corresponding Author**, Phone: 410-955-2789. Fax: 443-817-0990. mpomper@jhmi.edu.

ASSOCIATED CONTENT

Supporting Information

HPLC conditions and traces for the final compounds, ligated to the commercial and previously reported NIR dyes used herein, are provided: 800CW-**1**; 800CW-**2**; 800CW-**3**; 800RS-**1**; 800RS-**2**; 800RS-**3**; ICG-**1**; ICG-**2**; ICG-**3**; Cy7-**1**; Cy7-**2**; Cy7-**3**; Cy5.5-**1**; Cy5.5-**2**; Cy5.5-**3**. This material is available free of charge via the Internet at http://pubs.acs.org.

The authors declare no competing financial interest.

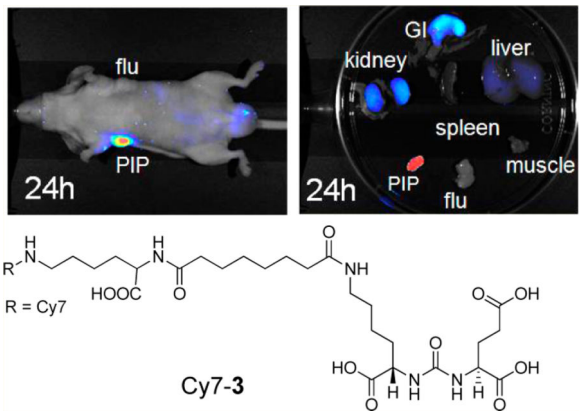

INTRODUCTION

The National Cancer Institute estimates 241 740 new cases and 28 170 new deaths from prostate cancer (PCa) in 2012.[1] PCa is the second leading cause of cancer-related death in men. Surgery is the most commonly used treatment for clinically localized PCa and provides a survival advantage compared to watchful waiting.[2] A pressing issue in surgery for PCa is the assurance of a complete resection of the tumor, namely, a negative surgical margin. A positive surgical margin necessitates adjuvant radiation therapy, which is required in up to 27.8% of patients[3] compared to 9.1% of men undergoing radical retropubic prostatectomy. Given that currently more than 50 000 radical prostatectomies are performed annually, these statistics would suggest that more than 9000 men are undergoing unnecessary adjuvant radiation therapy.[4] Given that such radiation therapy costs in excess of $25 000 per patient, the estimated cost of preventable positive margins is at least $225 M annually.

Local tumor invasion can be difficult to assess pre- and even intraoperatively, but its detection during surgery can be augmented through the use of fluorescent dyes that home to tumor in conjunction with an excitation laser and camera that are tuned to the excitation and emission wavelengths of the dye employed.[5–7] While such intraoperative tumor detection has been performed using nontargeted agents,[8] targeted agents are coming online.[9,10] Because of superior tissue penetration and less interference from the presence of blood in the surgical field, dyes with emission wavelengths in the near-infrared (NIR) region of the spectrum (650–900 nm) are generally employed for this purpose.[11] Because of its abundant expression on the surface of PCa[12,13] as well as within most solid tumor neovasculature,[14–17] we have developed a series of NIR-emitting dyes that target the prostate-specific membrane antigen (PSMA).

We and others have synthesized a variety of low-molecular-weight PSMA-targeting radiotracers to enable imaging of PCa, with several such agents currently in the clinic.[18–21] Optical agents have also been synthesized,[22–24] and we have previously tested one such compound in mice to good effect.[9] While a variety of radiolabeled PSMA-targeting antibodies have been used for tumor imaging,[25–27] we prefer agents of low molecular weight due to more tractable pharmacokinetics, namely, more rapid washout from nontarget sites enabling imaging within hours rather than days of administration.

NIR-emitting optical dyes are relatively large organic molecules with extended conjugation, which presents two potential difficulties for target acquisition in vivo: (1) steric hindrance when linked to small affinity agents, such as the ureas present in many of the above mentioned PSMA inhibitors; and (2) poor pharmacokinetics. Recently, we reported the preparation and evaluation in vivo of YC-27 (800CW-**3**), which contains a lysine–suberate linker between the dye (IRDye800CW, LI-COR Biosciences, Lincoln, NE) and the PSMA targeting urea.[9] With 800CW-**3** we were able to visualize a PSMA+ tumor xenograft by optical imaging, demonstrating that with a long lysine–suberate linking moiety, i.e., a long linker, PSMA inhibitors containing bulky groups will still bind to the target. Here, we extend this work by synthesizing and testing a series of PSMA-targeted NIR fluorescent agents, each containing either no linker, or one of two different linking groups that have different pharmacokinetic implications for imaging in vivo.

EXPERIMENTAL PROCEDURES

Chemistry

General Methods—All chemicals and solvents were purchased from either Sigma-Aldrich (Milwaukee, WI) or Fisher Scientific (Pittsburgh, PA). The *N*-hydroxysuccinimide (NHS) esters of IRDye800CW and IRDye800RS were purchased from LI-COR Biosciences. The *N*-hydroxysulfosuccinimide ester of ICG derivative (ICG-sulfo-OSu) was purchased from DOJINDO Molecular Technologies (Rockville, MD). The NHS esters of Cy7 and Cy5.5 were purchased from GE Healthcare (Piscataway, NJ). ^{1}H NMR spectra were obtained on a Bruker Avance 400 MHz Spectrometer (Billerica, MA). Mass spectra were obtained on a Bruker Esquire 3000 plus system (ESI) or an Applied Biosystems Voyager DE-FTR MALDI-TOF (Foster City, CA). High-performance liquid chromatography (HPLC) purifications were performed on a Waters 625 LC system (Milford, MA) or a Varian Prostar System (Varian Medical Systems, Palo Alto, CA). Optical images were obtained using the Pearl Impulse Imager (LI-COR Biosciences, Lincoln, NE) and a Xenogen IVIS Spectrum (Caliper Life Sciences, Hopkinton, MA). HPLC traces of all of the final compounds are available in the Supporting Information.

Synthesis of (S)-2-(3-((S)-5-Amino-1-carboxypentyl)-ureido)pentanedioic Acid (1)—To a solution of (10*S*,14*S*)-tris(4-methoxybenzyl) 2,2-dimethyl-4,12-dioxo-3-oxa-5,11,13-triazahexadecane-10,14,16-tricarboxylate **4**[28] (0.264 g, 0.033 mmol) a solution of 3% anisole in TFA (1 mL) was added and the mixture was reacted at room temperature for 20 min, then concentrated on a rotary evaporator. The crude material was purified by HPLC [Econosphere C18, 10 μm, 250 × 10 mm, H_2O/CH_3CN/TFA (92/8/0.1), 4 mL/min] to afford 0.108 g (74%) of **1** (retention time = 4 min). ^{1}H NMR (400 MHz, D_2O) δ 4.17–4.25 (m, 2H), 2.94–2.98 (m, 2H), 2.46–2.50 (m, 2H), 2.11–2.19 (m, 1H), 1.80–1.98 (m, 2H), 1.61–1.73 (m, 3H), 1.40–1.49 (m, 2H). ^{13}C NMR (400 MHz, D_2O): δ 176.9, 176.8, 176.2, 163.0, 162.7, 162.3, 162.0, 158.8, 120.2, 117.3, 114.1, 111.5, 52.7, 52.4, 38.8, 30.0, 29.7, 25.8, 25.7, 21.5. ESI-Mass calcd for $C_{12}H_{22}N_3O_7$ $[M]^+$ 320.2, found 320.0.

Synthesis of 800CW-1—To a solution of **1** (0.5 mg, 1.15 μmol) in DMSO (0.1 mL) was added *N*,*N*-diisopropylethylamine (0.002 mL, 11.5 μmol), followed by the NHS ester of

IRDye800CW (0.3 mg, 0.26 μmol). After 2 h at room temperature, the reaction mixture was purified by HPLC (Econosphere C18, 5 μm, 150 × 4.6 mm; mobile phase, A = 0.1% TFA in H_2O, B = 0.1% TFA in CH_3CN; gradient, 0 min = 5% B, 5 min = 5% B, 45 min = 100% B; flow rate, 1 mL/min) to afford 0.2 mg (60%) of 800CW-**1** (retention time = 15 min). ESI-Mass calcd for $C_{58}H_{74}N_5O_{21}S_4$ $[M]^+$ 1304.4, found 1303.8.

Synthesis of 800RS-1—To a solution of **1** (0.2 mg, 0.46 μmol) in DMSO (0.05 mL) was added *N*,*N*-diisopropylethylamine (0.002 mL, 11.5 μmol), followed by the NHS ester of IRDye800RS (0.2 mg, 0.21 μmol). After 2 h at room temperature, the reaction mixture was purified by HPLC as described for 800CW-**1** to afford 0.2 mg (84%) of 800RS-**1** (retention time = 23 min). ESI-Mass calcd for $C_{58}H_{73}N_5O_{15}S_2$ $[M]^+$ 1143.5, found 572.5 $[M+H]^{2+}$, 1144.0 $[M]^+$.

Synthesis of ICG-1—To a solution of **1** (0.2 mg, 0.46 μmol) in DMSO (0.1 mL) was added *N*,*N*-diisopropylethylamine (0.002 mL, 11.5 μmol), followed by ICG-sulfo-OSu (0.3 mg, 0.32 μmol). After 2 h at room temperature, the reaction mixture was purified by HPLC as described for 800CW-**1** to afford 0.2 mg (60%) of ICG-**1** (retention time = 24 min). ESI-Mass calcd for $C_{57}H_{69}N_5O_{11}S$ $[M]^+$ 1031.5, found 516.5 $[M+H]^{2+}$, 1032.0 $[M]^+$.

Synthesis of Cy7-1—To a solution of **1** (0.5 mg, 1.15 μmol) in DMSO (0.1 mL) was added *N*,*N*-diisopropylethylamine (0.002 mL, 11.5 μmol), followed by the NHS ester of Cy7 (0.3 mg, 0.37 μmol). After 2 h at room temperature, the reaction mixture was purified by HPLC as described for 800CW-**1** to afford 0.2 mg (55%) of Cy7-**1** (retention time = 16 min). ESI-Mass calcd for $C_{47}H_{61}N_5O_{14}S_2$ $[M]^+$ 983.4, found 492.5 $[M+H]^{2+}$, 984.0 $[M]^+$.

Synthesis of Cy5.5-1—To a solution of **1** (0.5 mg, 1.15 μmol) in DMSO (0.1 mL) was added *N*,*N*-diisopropylethylamine (0.002 mL, 11.5 μmol), followed by the NHS ester of Cy5.5 (0.3 mg, 0.27 μmol). After 2 h at room temperature, the reaction mixture was purified by HPLC as described for 800CW-**1** to afford 0.2 mg (62%) of Cy5.5-**1** (retention time = 14 min). ESI-Mass calcd for $C_{53}H_{63}N_5O_{20}S_4$ $[M]^+$ 1217.3, found 609.4 $[M+H]^{2+}$, 1217.7 $[M]^+$.

Synthesis of (14S,18S)-1-Amino-8,16-dioxo-3,6-dioxa-9,15,17-triazaicosane-14,18,20-tricarboxylic Acid (2)—To the tosylate salt of (*S*)-5-(3-((*S*)-1,5-bis((4-methoxybenzyl)oxy)-1,5-dioxopentan-2-yl)ureido)-6-((4-methoxybenzyl)oxy)-6-ox-ohexan-1-aminium **5**[28,29] (0.103 g, 0.121 mmol) in DMF (2 mL) was added Boc-NH$(CH_2CH_2O)_2CH_2COOH$ (0.060 g, 0.135 mmol) and TBTU (0.040g, 0.125 mmol), followed by *N*,*N*-diisopropylethylamine (0.042 mL, 0.241 mmol). After stirring overnight at room temperature, the solvent was evaporated on a rotary evaporator. The crude material was purified by silica gel column chromatography using methanol/methylene chloride (5:95) to give 0.101 g of (14S,18S)-tris(4-methoxybenzyl) 1-amino-8,16-dioxo-3,6-dioxa-9,15,17-triazaicosane-14,18,20-tricarboxylate, **6** in 90% yield. MALDI-TOF Mass calcd for $C_{47}H_{64}N_4NaO_{15}$ $[M+Na]^+$ 947.4, found 947.1. Compound **6** was dissolved in a solution of 3% anisole in TFA (1 mL), allowed to react at room temperature for 10 min, and then concentrated. The crude material was purified by HPLC

[Econosphere C18, 10 μm, 250 × 10 mm, H_2O/CH_3CN/TFA (92/8/0.1), 4 mL/min] to afford 0.035 g (57%) of **2** (retention time = 11 min). ^{1}H NMR (400 MHz, D_2O) δ 4.17–4.21 (m, 1H), 4.10–4.13 (m, 1H), 4.00 (s, 2H), 3.67–3.71 (m, 6H), 3.14–3.20 (m, 4H), 2.43–2.46 (m, 2H), 2.08–2.13 (m, 1H), 1.87–1.93 (m, 1H), 1.76–1.79 (m, 1H), 1.63–1.67 (m, 1H), 1.45–1.50 (m, 2H), 1.33–1.40 (m, 2H). ^{13}C NMR (400 MHz, D_2O): δ 176.9, 176.8, 176.0, 171.7, 163.0, 162.7, 162.3, 162.0, 158.8, 117.3, 114.4, 69.8, 69.0, 65.9, 52.8, 52.2, 38.6, 38.1, 30.1, 29.6, 27.3, 25.8, 21.5. ESI-Mass calcd for $C_{18}H_{33}N_4O_{10}$ $[M]^+$ 465.2, found 465.2.

Synthesis of 800CW-2—To a solution of compound **2** (0.3 mg, 0.52 μmol) in DMSO (0.05 mL) was added *N*,*N*-diisopropylethylamine (0.002 mL, 11.5 μmol), followed by the NHS ester of IRDye800CW (0.2 mg, 0.17 μmol). After 2 h at room temperature, the reaction mixture was purified by HPLC (Econosphere C18, 5 μm, 150 × 4.6 mm mobile phase, A = 50 mM triethylamine acetate buffer (pH 6.0), B = CH_3CN; gradient, 0 min = 0% B, 5 min = 0% B, 45 min = 100% B; flow rate, 1 mL/min) to afford 0.2 mg (80%) of 800CW-**2** (retention time = 22 min). ESI-Mass calcd for $C_{64}H_{84}N_6O_{24}S_4$ $[M]^+$ 1448.4, found 1448.7.

Synthesis of 800RS-2—To a solution of **2** (0.3 mg, 0.52 μmol) in DMSO (0.05 mL) was added *N*,*N*-diisopropylethylamine (0.002 mL, 11.4 μmol), followed by the NHS ester of IRDye800RS (0.2 mg, 0.21 μmol). After 2 h at room temperature, the reaction mixture was purified by HPLC as in 800CW-**2** to afford 0.2 mg (75%) of 800RS-**2** (retention time = 28 min). ESI-Mass calcd for $C_{64}H_{84}N_6O_{18}S_2$ $[M]^+$ 1288.5, found 1288.9.

Synthesis of ICG-2—To a solution of **2** (0.5 mg, 0.86 μmol) in DMSO (0.1 mL) was added *N*,*N*-diisopropylethylamine (0.002 mL, 11.5 μmol), followed by ICG-sulfo-OSu (0.3 mg, 0.32 μmol). After 2 h at room temperature, the reaction mixture was purified by HPLC as described for 800CW-**1** to afford 0.2 mg (53%) of ICG-**2** (retention time = 26 min). ESI-Mass calcd for $C_{63}H_{80}N_6O_{14}S$ $[M]^+$ 1176.5, found 589.1 $[M+H]^{2+}$, 1177.1 $[M]^+$.

Synthesis of Cy7-2—To a solution of **2** (0.5 mg, 0.86 μmol) in DMSO (0.1 mL) was added *N*,*N*-diisopropylethylamine (0.002 mL, 11.5 μmol), followed by the NHS ester of Cy7 (0.2 mg, 0.24 μmol). After 2 h at room temperature, the reaction mixture was purified by HPLC as in 800CW-**1** to afford 0.2 mg (72%) of Cy7-**2** (retention time = 17 min). ESI-Mass calcd for $C_{53}H_{72}N_6O_{17}S_2$ $[M]^+$ 1128.4, found 565.0 $[M+H]^{2+}$, 1129.0 $[M]^+$.

Synthesis of Cy5.5-2—To a solution of **2** (0.5 mg, 0.86 μmol) in DMSO (0.1 mL) was added *N*,*N*-diisopropylethylamine (0.002 mL, 11.5 μmol), followed by the NHS ester of Cy5.5 (0.2 mg, 0.18 μmol). After 2 h at room temperature, the reaction mixture was purified by HPLC as in 800CW-**1** to afford 0.2 mg (83%) of Cy5.5-**2** (retention time = 13 min). ESI-Mass calcd for $C_{59}H_{74}N_6O_{23}S_4$ $[M]^+$ 1362.4, found 681.9 $[M+H]^{2+}$, 1362.7 $[M]^+$.

Synthesis of 800RS-3—To a solution of **3**[9] (0.3 mg, 0.42 μmol) in DMSO (0.1 mL) was added *N*,*N*-diisopropylethylamine (0.002 mL, 11.5 μmol), followed by the NHS ester of IRDye800RS (0.3 mg, 0.31 μmol). After 2 h at room temperature, the reaction mixture was purified by HPLC (column, Econosphere C18 5 μ, 150 × 4.6 mm; retention time, 27 min; mobile phase, A = 0.1% TFA in H_2O, B = 0.1% TFA in CH_3CN; gradient, 0 min = 0% B, 5 min = 0% B, 45 min = 100% B; flow rate, 1 mL/min) to afford 0.3 mg (67%) of 800RS-**3**

(retention time = 27 min). ESI-Mass calcd for $C_{72}H_{97}N_7O_{19}S_2$ $[M]^+$ 1427.6, found 714.4 $[M+H]^{2+}$, 1427.8 $[M]^+$.

Synthesis of ICG-3—To a solution of **3** (0.5 mg, 0.71 μmol) in DMSO (0.1 mL) was added *N*,*N*-diisopropylethylamine (0.002 mL, 11.5 μmol), followed by ICG-Sulfo-OSu (0.3 mg, 0.32 μmol). After 2 h at room temperature, the reaction mixture was purified by HPLC as in 800RS-**3** to afford 0.3 mg (71%) of ICG-**3** (retention time = 32 min). ESI-Mass calcd for $C_{71}H_{93}N_7O_{15}S$ $[M]^+$ 1315.6, found 1316.0 $[M]^+$.

Synthesis of Cy7-3—To a solution of **3** (0.5 mg, 0.71 μmol) in DMSO (0.1 mL) was added *N*,*N*-diisopropylethylamine (0.002 mL, 11.5 μmol), followed by the NHS ester of Cy7 (0.5 mg, 0.61 μmol). After 2 h at room temperature, the reaction mixture was purified by HPLC as in 800RS-**3** to afford 0.5 mg (64%) of Cy7-**3** (retention time = 19 min). ESI-Mass calcd for $C_{61}H_{85}N_7O_{18}S_2$ $[M]^+$ 1267.5, found 634.5 $[M+H]^{2+}$, 1267.9 $[M]^+$.

Synthesis of Cy5.5-3—To a solution of **3** (0.5 mg, 0.71 μmol) in DMSO (0.1 mL) was added *N*,*N*-diisopropylethylamine (0.002 mL, 11.5 μmol), followed by the NHS ester of Cy5.5 (0.5 mg, 0.44 μmol). After 2 h at room temperature, the reaction mixture was purified by HPLC as in 800RS-**3** to afford 0.6 mg (90%) of Cy5.5-**3** (retention time = 18 min). ESI-Mass calcd for $C_{67}H_{87}N_7O_{24}S_4$ $[M]^+$ 1501.5, found 751.4 $[M+H]^{2+}$, 1501.6 $[M]^+$.

Biology

In Vitro PSMA Inhibition Assay—The PSMA binding affinities of the dye–urea conjugates for PSMA were measured using the *N*-acetylated-α-linked acidic dipeptidase (NAALADase) assay, as previously described.[30,31] PSMA is known also as glutamate carboxypeptidase II (GCPII), or NAALADase.[32,33] A reaction mixture (total volume of 50 μL) containing [^{3}H]*N*-acetyl-aspartylglutamate ([^{3}H]NAAG, 30 nM, 1850 GBq/mmol) and human recombinant GCPII (40 pM final) in Tris-HCl (pH 7.4, 40 mM) containing 1 mM $CoCl_2$ was used. The reaction was carried out at 37 °C for 15 min and stopped with ice-cold sodium phosphate buffer (pH 7.4, 0.1 M, 50 μL). Blanks were obtained by incubating the reaction mixture in the presence of 2-phosphonomethyl pentanedioic acid (2-PMPA, 1 μM final), a selective and potent inhibitor of PSMA.[32] Dye-urea conjugates and controls were tested at log-unit final concentrations that ranged from 100 μM to < fM. A 90 μL aliquot from each terminated reaction was transferred to a well in a 96-well spin column containing AG1 × 8 ion-exchange resin. The plate was centrifuged at 1500 rpm for 5 min using a Beckman GS-6R centrifuge (Beckman Coulter, Inc., Brea, CA) equipped with a PTS-2000 rotor. [^{3}H]NAAG bound to the resin and [^{3}H]-glutamate eluted in the flowthrough. Columns were then washed twice with formate (1 M, 90 μL) to ensure complete elution of [^{3}H]glutamate. The flowthrough and the washes were collected in a deep 96-well block. From each well with a total volume of 270 μL, a 200 μL aliquot was transferred to its respective well in a solid scintillator-coated 96-well plate (Packard, Meriden, CT) and dried to completion. The radioactivity corresponding to [^{3}H]glutamate was determined with a scintillation counter (Topcount NXT, Packard, counting efficiency 80%). IC_{50} curves were generated from CPM results, by use of both *Microsoft Office Excel 2007 and GraphPad Prism 5* programs, with K_i values derived from the IC_{50} values.[34]

Cell Lines and Tumor Models—PSMA+ PC3 PIP and PSMA nonexpressing PC3 flu cell lines were originally a gift from Warren Heston (Cleveland Clinic Foundation[35]). Cells were cultured in RPMI 1640 medium (Mediatech, Manassas, VA) containing 10% FBS (Sigma) and 1% penicillin–streptomycin (Mediatech) in a humidified incubator under 5% CO_2 at 37 °C. Cells were cultured to 80% confluence and then trypsinized and collected. Two million cells each of PSMA+ PC3 PIP and PSMA- PC3 flu were resuspended in 0.1 mL PBS (Mediatech) and injected subcutaneously (s.c.) into 4–6-week-old male athymic nude mice (NCI, Frederick, MD) in the upper right and left flanks. Mice were used in imaging studies when tumors reached 3–5 mm in diameter.

In Vivo Imaging and Ex Vivo Biodistribution—In vivo images with compounds Cy5.5-**1**, Cy5.5-**2**, and Cy5.5-**3** were acquired on the IVIS Spectrum using an excitation wavelength of 675 nm and detection of the emission wavelength at 720 nm. The exposure time for each image acquisition was 1 s. Images were scaled to the same maximum intensity using the supplier's software.

Compounds containing 800CW, 800RS, ICG derivative, and Cy7 as fluorophores were imaged using the Pearl Impulse Imager. The Pearl imager is a dedicated fluorescence imaging instrument for mice and has fixed excitation wavelengths of 685 and 785 nm and emission wavelengths of 700 and 800 nm, respectively, as well as a white-light overlay. For in vivo studies, stock solutions (~1 mM) of dye–urea conjugates were prepared in H_2O (compounds containing 800CW, 800RS, Cy5.5, and Cy7) or DMSO (compounds containing the ICG derivative) and were diluted with PBS for injection. After image acquisition at baseline (preinjection), each mouse was injected intravenously with 1 nmol of dye–urea conjugate and images were acquired at 5 min, 1 h, 4 h, and 24 h time points. Following the 24 h image, each mouse was sacrificed by cervical dislocation and tumor, muscle, liver, spleen, kidneys, and intestine were collected and assembled on a Petri dish for image acquisition. All images were scaled to the same maximum intensity for direct comparison. For quantification, regions of interest (ROI) were drawn over the organs displayed in ex vivo images ($n = 4$) and fluorescence signal intensity of the organs was calculated using the supplier's software. Signal intensity of the muscle was set as background for all calculations. For binding specificity (blocking) studies, Cy7-**3** was coinjected with 1 μmol of (*S*)-2-(3-((*S*)-1-carboxy-5-(4-iodobenzamido)-pentyl)ureido)pentanedioic acid (DCIBzL, a known high-affinity PSMA inhibitor[29]) and images were acquired at 1, 4, and 24 h postinjection.

RESULTS AND DISCUSSION

Chemical Synthesis

Compound 1 is urea containing both lysine and glutamate substituents (a lysine-glutamate urea). It was obtained after deprotection of the *tert*-butyloxycarbonyl (Boc) and the *p*-methoxybenzyl (PMB) groups from compound **4**[28] as outlined in Scheme 1. Compound **2** has a short poly(ethylene glycol) (PEG) linker. Compound **5**[28] was conjugated to Boc-$NH(CH_2CH_2O)_2CH_2COOH$ to give compound 6, which was then deprotected to provide compound **2**. Compound **3** has a lysine–suberate linker attached to the lysine–glutamate urea, and it was prepared as previously reported.[9]

The commercially available amine-reactive active esters of IRDye800CW, IRDye800RS, the indocyanine green (ICG) derivative, Cy7, or Cy5.5 with principal excitation/emission wavelengths at 774/789, 767/786, 768/804, 743/767, and 675/ 694 nm, respectively, were conjugated with **1**, **2**, and **3** to produce the dye–PSMA inhibitors shown in Figure 1. Conjugation of activated esters of the NIR dyes to **1–3** were completed at room temperature within 2 h. The yields for these conjugates ranged from 53% to 90%.

In Vitro PSMA Inhibition

The IC_{50} values of the conjugates were measured using the NAALADase assay[30,31] with results presented as K_i values in Table 1. The K_i values range from 1 to 700 pM, which is similar to other compounds of this class.[9,28,29,36] We observed a trend whereby agents with linkers, such as 800CW-**2**, ICG-**2**, Cy5.5-**2**, 800CW-**3**, ICG-**3**, and Cy5.5-**3**, had lower K_i values than their counterparts with no linkers (800CW-**1**, ICG-1, and Cy5.5-**1**). However, Cy7 conjugates did not follow this trend and exhibited similar high affinities independent of the linker. This may be due to the smaller size of Cy7 compared to Cy5.5 and ICG derivative and the greater flexibility of the polyene moiety in Cy7 compared to the cyclohexene containing polyene in 800CW and 800RS dyes. Both effects could increase the accessibility of the urea to the PSMA binding site.

NIR Imaging and Biodistribution

Among the five dyes tested in this study, only the Cy5.5–urea conjugates have excitation and emission wavelengths below 700 nm. Accordingly, imaging studies with Cy5.5-**1**, Cy5.5-**2**, and Cy5.5-**3** were undertaken on the Xenogen IVIS 200 system with excitation at 675 nm and emission at 720 nm. Figure 2 shows images at 24 h after injection of 1 nmol of Cy5.5-**1**, Cy5.5-**2**, and Cy5.5-**3** in mice with PSMA+ PC3 PIP and PSMA- PC3 flu tumors. All three compounds demonstrated high uptake within PSMA+ PC3 PIP tumors and little uptake in PSMA- PC3 flu tumors. The relative degree of observed PSMA+ PC3 PIP tumor uptake was in the order: Cy5.5-**3** > Cy5.5-**2** > Cy5.5-**1**. Renal uptake is due to high expression of PSMA within proximal renal tubules as well as to excretion, as previously shown.[37–39] Imaging of compounds containing 800CW, 800RS, the ICG derivative, and Cy7 as fluorophores were conducted using the Pearl Imager, which has a set excitation wavelength at 785 nm and emission at 800 nm. These dye–urea conjugates have excitation and emission wavelengths above 700 nm, which allow for better depth of light penetration than compounds that emit at lower wavelengths and minimal autofluorescence. Figure 3 shows typical whole body and excised organ imaging of mice with PSMA+ PC3 PIP and PSMA- PC3 flu tumors at 24 h after injection of 1 nmol of the 800CW, 800RS, the ICG derivative or Cy7-urea conjugates. All compounds demonstrated PSMA+ PC3 PIP tumor uptake with little PSMA- PC3 flu tumor uptake, indicating target selectivity in vivo.

These images also demonstrate that the choice of dye and linking group have significant effects on biodistribution. Intense fluorescence signals were observed in both tumor and kidneys for all three IRDye800CW conjugates (800CW-**1**, 800CW-**2**, and 800CW-**3**) with 800CW-**3** having much lower normal tissue uptake than the other two compounds. IRDye800RS has a similar structure, but with two less sulfonate groups compared to IRDye800CW. PSMA+ PIP tumor uptake was observed in all three 800RS–urea conjugates.

However, the fluorescence intensities were significantly lower than for the corresponding 800CW conjugates. Among those three 800RS–urea conjugates, 800RS-**3**, which has a lysine suberate linker, showed the highest PSMA+ PIP tumor uptake. Similarly, among the three ICG–urea conjugates, ICG-**3** gave the highest PSMA+ PIP tumor uptake. ICG-**3** also demonstrated higher PSMA+ PIP tumor uptake compared to kidney, which differs from 800CW-**3** and 800RS-**3**, which had roughly equivalent tumor and kidney uptake. Cy7-**2** and Cy7-**3** had significantly higher PSMA + PIP tumor uptake than uptake in kidneys. They also demonstrated the lowest normal tissue uptake comparing to the other compounds with the same linker. From this preliminary evaluation, we chose 800CW and Cy7 conjugates for further study, where the organs of 4 mice/agent were harvested and imaged at 24 h postadministration of imaging agent. Fluorescence intensity per organ is shown in Figure 4. In both the Cy7 series and the IRDye800CW series, the degree of PSMA+ PIP tumor uptake was 800CW-**3** or Cy7-**3** ≈ 800CW-**2** or Cy7-**2** > 800CW-**1** or Cy7-**1**, confirming the importance of the linker moiety for modifying pharmacokinetics. Tumor to kidney ratios for Cy7-**2** and Cy7-**3** were higher than for 800CW-**2** and 800CW-**3**. The fluorescence intensities of all organs except the gastrointestinal tract for Cy7 conjugates were lower than for the corresponding 800CW conjugates. This is most likely because the Pearl Imager has a fixed excitation maximum at 785 nm and collects emission at 820 nm, which is further from the excitation and emission maxima of Cy7 (743/767) than those for IRDye800CW (774/789).

In order to demonstrate the PSMA-binding specificity of the PSMA inhibitor–dye conjugates, DCIBzL was coadministered with Cy7-**3**. As shown in Figure 5, all emission from the PSMA + target tumor was blocked with concurrent DCIBzL administration, indicating specific binding. The excised organ imaging results are consistent with the in vivo images.

The active site of PSMA possesses two binding sites, comprising a pharmacophore (S1′) site and an amphiphilic, nonpharmacophore (S1) site.[40] The S1′ site is generated by amino acid residues highly sensitive to structural modification of potential ligands, demonstrating a strong preference for glutamate or glutamate-like residues. Compared to the S1′ site, the S1 site is more promiscuous. A tunnel-like region (~20 Å) linked to the S1 site is projected toward the surface of the enzyme. Utilizing the tunnel region, we have attached bulky chelated metals to the urea-based specificity-conferring moiety through a long linker to maintain the chelated metal entirely outside the protein. In so doing, we have produced a small array of PSMA-targeted radiotracers capable of imaging PSMA in experimental models of prostate cancer.[28,36,41] Similarly, by attaching bulky fluorophores to the urea inhibitors through a linker, such as in dye-**2** or dye-**3** conjugates, the fluorophores can be situated outside of the active site, allowing maximum interaction with the urea-based specificity conferring portion of the agent. This effect is most noticeable in the higher tumor uptake demonstrated by 800RS-**2**, 800RS-**3**, ICG-**2**, ICG-**3**, and Cy5.5-**3** compared to dye–1 conjugates 800RS-**1**, ICG-**1**, and Cy5.5-**1**.

Recently, Nakajima et al. used the anti-PSMA antibody J591 conjugated to ICG to visualize PSMA+ tumors in whole mice at up to 10 days after administration.[10] We and others have focused on developing low-molecular-weight optical imaging agents for PSMA, in part to avoid the longer biological half-lives of antibody-based methods, to enable imaging at

shorter times after administration.[9,23,24,42–44] However, to date most such low-molecular-weight agents have only been used in vitro. Humblet et al. reported in vivo imaging of PSMA-binding NIR-emitting phosphonate derivatives; however, at 20 s, the time of maximum PSMA-positive tumor uptake, the tumor to background ratio was less than 2.[24] Previously, we were able to image PSMA+ tissues in experimental models of prostate cancer using the targeted, IRDye800CW-based agent, YC-27 (800CW-**3**).[9] Here, we used the same urea-based targeting moiety but expanded to the small series reported, investigating the pharmacokinetic effects of different linkers and fluorophores.

CONCLUSION

Compounds **2** and **3**, which contain PEG and lysine-suberate linkers, respectively, provide useful scaffolds for optical imaging of PSMA. Although IRDye800CW and Cy7 conjugates 800CW-**2**, 800CW-**3**, Cy7-**2**, and Cy7-**3** demonstrated high, PSMA-specific uptake in vivo at 24 h postinjection, the exact choice of dye for intraoperative imaging will depend upon the specifications of the camera used for detection in the operating suite. Nevertheless, this small series demonstrates that a variety of dyes with different absorption and emission spectra can be accommodated.

Supplementary Material

Refer to Web version on PubMed Central for supplementary material.

Acknowledgments

We thank CA134675 and the AdMeTech Foundation for financial support and Dr. Ron Rodriguez for helpful discussions.

ABBREVIATIONS

NIR	near-infrared
ICG	indocyanine green
PSMA	prostate-specific membrane antigen
NAAG	*N*-acetylaspartyl glutamate
NAALADase	*N*-acetylated-α-linked-acidic dipeptidase
Boc	*tert*-butyloxycarbonyl
PMB	*p*-methoxybenzyl
PEG	poly-(ethylene glycol)
NHS	*N*-hydroxysuccinimide
DCIBzL	(*S*)-2-(3-((*S*)-1-carboxy-5-(4-iodobenzamido)pentyl)ureido)-pentanedioic acid

REFERENCES

1. Siegel R, Naishadham D, Jemal A. Cancer statistics, 2012. Ca— Cancer J. Clin. 2012; 62:10–29. [PubMed: 22237781]
2. Bill-Axelson A, Holmberg L, Ruutu M, Garmo H, Stark JR, Busch C, Nordling S, Haggman M, Andersson SO, Bratell S, Spangberg A, Palmgren J, Steineck G, Adami HO, Johansson JE. Radical prostatectomy versus watchful waiting in early prostate cancer. N. Engl. J. Med. 2011; 364:1708–1717. [PubMed: 21542742]
3. National Cancer Institute. Surveillance Epidemiology and End Results (SEER). 2008. http://seer.cancer.gov/data/
4. Hu JC, Wang Q, Pashos CL, Lipsitz SR, Keating NL. Utilization and outcomes of minimally invasive radical prostatectomy. J. Clin. Oncol. 2008; 26:2278–2284. [PubMed: 18467718]
5. Gioux S, Choi HS, Frangioni JV. Image-guided surgery using invisible near-infrared light: fundamentals of clinical translation. Mol. Imaging. 2010; 9:237–255. [PubMed: 20868625]
6. Frangioni JV. New technologies for human cancer imaging. J. Clin. Oncol. 2008; 26:4012–4021. [PubMed: 18711192]
7. Ye Y, Bloch S, Xu B, Achilefu S. Design, synthesis, and evaluation of near infrared fluorescent multimeric RGD peptides for targeting tumors. J. Med. Chem. 2006; 49:2268–2275. [PubMed: 16570923]
8. Schaafsma BE, Mieog JS, Hutteman M, van der Vorst JR, Kuppen PJ, Lowik CW, Frangioni JV, van de Velde CJ, Vahrmeijer AL. The clinical use of indocyanine green as a near-infrared fluorescent contrast agent for image-guided oncologic surgery. J. Surg. Oncol. 2011; 104:323–332. [PubMed: 21495033]
9. Chen Y, Dhara S, Banerjee SR, Byun Y, Pullambhatla M, Mease RC, Pomper MG. A low molecular weight PSMA-based fluorescent imaging agent for cancer. Biochem. Biophys. Res. Commun. 2009; 390:624–629. [PubMed: 19818734]
10. Nakajima T, Mitsunaga M, Bander NH, Heston WD, Choyke PL, Kobayashi H. Targeted, activatable, in vivo fluorescence imaging of prostate-specific membrane antigen (PSMA) positive tumors using the quenched humanized J591 antibody-indocyanine green (ICG) conjugate. Bioconjugate Chem. 2011; 22:1700–1705.
11. Solomon M, Liu Y, Berezin MY, Achilefu S. Optical imaging in cancer research: basic principles, tumor detection, and therapeutic monitoring. Medical Principles and Practice: International Journal of the Kuwait University, Health Science Centre. 2011; 20:397–415.
12. Silver DA, Pellicer I, Fair WR, Heston WD, Cordon-Cardo C. Prostate-specific membrane antigen expression in normal and malignant human tissues. Clin. Cancer Res. 1997; 3:81–85. [PubMed: 9815541]
13. Ghosh A, Heston WD. Tumor target prostate specific membrane antigen (PSMA) and its regulation in prostate cancer. J. Cell. Biochem. 2004; 91:528–539. [PubMed: 14755683]
14. Baccala A, Sercia L, Li J, Heston W, Zhou M. Expression of prostate-specific membrane antigen in tumor-associated neovasculature of renal neoplasms. Urology. 2007; 70:385–390. [PubMed: 17826525]
15. Chang SS, O'Keefe DS, Bacich DJ, Reuter VE, Heston WD, Gaudin PB. Prostate-specific membrane antigen is produced in tumor-associated neovasculature. Clin. Cancer Res. 1999; 5:2674–2681. [PubMed: 10537328]
16. Haffner MC, Kronberger IE, Ross JS, Sheehan CE, Zitt M, Muhlmann G, Ofner D, Zelger B, Ensinger C, Yang XJ, Geley S, Margreiter R, Bander NH. Prostate-specific membrane antigen expression in the neovasculature of gastric and colorectal cancers. Hum. Pathol. 2009; 40:1754–1761. [PubMed: 19716160]
17. Milowsky MI, Nanus DM, Kostakoglu L, Sheehan CE, Vallabhajosula S, Goldsmith SJ, Ross JS, Bander NH. Vascular targeted therapy with anti-prostate-specific membrane antigen monoclonal antibody J591 in advanced solid tumors. J. Clin. Oncol. 2007; 25:540–547. [PubMed: 17290063]
18. Cho SY, Gage KL, Mease RC, Senthamizhchelvan S, Holt DP, Kwanisai-Jeffrey A, Endres CJ, Dannals RF, Sgouros G, Lodge MA, Eisenberger MA, Rodriguez R, Carducci MA, Rojas C, Slusher BS, Kozikowski AP, Pomper MG. Biodistribution, tumor detection and radiation

dosimetry of *N*-[N-[(S)-1,3-Dicarboxypropyl]carbamoyl]-4-18F-fluorobenzyl-L-cysteine (18F-DCFBC), a low molecular weight inhibitor of PSMA, in patients with metastatic prostate cancer. J. Nucl. Med. 2012; 53:1883–1891. [PubMed: 23203246]

19. Barrett JS, LaFrance N, Coleman RE, Goldsmith SJ, Stubbs JB, Petry NA, Vallabhajosula S, Maresca KP, Femia FJ, Babich JW. Targeting metastatic prostate cancer [PCa] in patients with 123I-MIP1072 & 123I-MIP1095. J. Nucl. Med. 2009; 50(Suppl):136.
20. Babich J, Coleman RE, Van Heertum R, Vallabahajosula S, Goldsmith S, Osborne J, Slawin K, Joyal J. Small molecule inhibitors of prostate specific membrane antigen (PSMA) for SPECT: Summary of phase I studies in patients with prostate cancer (PCa). J. Nucl. Med. 2012; 53(Suppl): 55. [PubMed: 22128324]
21. Afshar-Oromieh A, Haberkorn U, Eder M, Eisenhut M, Zechmann CM. [68Ga]Gallium-labelled PSMA ligand as superior PET tracer for the diagnosis of prostate cancer: comparison with 18F-FECH. Eur. J. Nucl. Med. Mol. Imaging. 2012; 39:1085–1086. [PubMed: 22310854]
22. Kularatne SA, Wang K, Santhapuram HK, Low PS. Prostate-specific membrane antigen targeted imaging and therapy of prostate cancer using a PSMA inhibitor as a homing ligand. Mol. Pharm. 2009; 6:780–789. [PubMed: 19361233]
23. Liu T, Wu LY, Hopkins MR, Choi JK, Berkman CE. A targeted low molecular weight near-infrared fluorescent probe for prostate cancer. Bioorg. Med. Chem. Lett. 2010; 20:7124–7126. [PubMed: 20947349]
24. Humblet V, Lapidus R, Williams LR, Tsukamoto T, Rojas C, Majer P, Hin B, Ohnishi S, De Grand AM, Zaheer A, Renze JT, Nakayama A, Slusher BS, Frangioni JV. High-affinity near-infrared fluorescent small-molecule contrast agents for in vivo imaging of prostate-specific membrane antigen. Mol. Imaging. 2005; 4:448–462. [PubMed: 16285907]
25. Elsasser-Beile U, Reischl G, Wiehr S, Buhler P, Wolf P, Alt K, Shively J, Judenhofer MS, Machulla HJ, Pichler BJ. PET imaging of prostate cancer xenografts with a highly specific antibody against the prostate-specific membrane antigen. J. Nucl. Med. 2009; 50:606–611. [PubMed: 19289418]
26. Bander NH, Trabulsi EJ, Kostakoglu L, Yao D, Vallabhajosula S, Smith-Jones P, Joyce MA, Milowsky M, Nanus DM, Goldsmith SJ. Targeting metastatic prostate cancer with radiolabeled monoclonal antibody J591 to the extracellular domain of prostate specific membrane antigen. J. Urol. 2003; 170:1717–1721. [PubMed: 14532761]
27. Yao D, Trabulsi EJ, Kostakoglu L, Vallabhajosula S, Joyce MA, Nanus DM, Milowsky M, Liu H, Goldsmith SJ. The utility of monoclonal antibodies in the imaging of prostate cancer. Semin. Urol. Oncol. 2002; 20:211–218. [PubMed: 12215974]
28. Banerjee SR, Foss CA, Castanares M, Mease RC, Byun Y, Fox JJ, Hilton J, Lupold SE, Kozikowski AP, Pomper MG. Synthesis and evaluation of technetium-99m- and rhenium-labeled inhibitors of the prostate-specific membrane antigen (PSMA). J. Med. Chem. 2008; 51:4504–4517. [PubMed: 18637669]
29. Chen Y, Foss CA, Byun Y, Nimmagadda S, Pullambahatla M, Fox JJ, Castanares M, Lupold SE, Babich JW, Mease RC, Pomper MG. Radiohalogenated prostate-specific membrane antigen (PSMA)-based ureas as imaging agents for prostate cancer. J. Med. Chem. 2008; 51:7933–7943. [PubMed: 19053825]
30. Robinson MB, Blakely RD, Couto R, Coyle JT. Hydrolysis of the brain dipeptide *N*-acetyl-L-aspartyl-L-glutamate. Identification and characterization of a novel *N*-acetylated alpha-linked acidic dipeptidase activity from rat brain. J. Biol. Chem. 1987; 262:14498–14506. [PubMed: 3667587]
31. Rojas C, Frazier ST, Flanary J, Slusher BS. Kinetics and inhibition of glutamate carboxypeptidase II using a microplate assay. Anal. Biochem. 2002; 310:50–54. [PubMed: 12413472]
32. Jackson PF, Cole DC, Slusher BS, Stetz SL, Ross LE, Donzanti BA, Trainor DA. Design, synthesis, and biological activity of a potent inhibitor of the neuropeptidase *N*-acetylated alpha-linked acidic dipeptidase. J. Med. Chem. 1996; 39:619–622. [PubMed: 8558536]
33. Foss CA, Mease RC, Cho SY, Kim HJ, Pomper MG. GCPII imaging and cancer. Curr. Med. Chem. 2012; 19:1346–1359. [PubMed: 22304713]

34. Cheng Y, Prusoff WH. Relationship between the inhibition constate (K1) and the concentration of inhibitor which causes 50% inhibition (I50) of an enzymatic reaction. Biochem. Pharmacol. 1973; 22:3099–3108. [PubMed: 4202581]
35. Ghosh A, Wang X, Klein E, Heston WD. Novel role of prostate-specific membrane antigen in suppressing prostate cancer invasiveness. Cancer Res. 2005; 65:727–731. [PubMed: 15705868]
36. Banerjee SR, Pullambhatla M, Byun Y, Nimmagadda S, Foss CA, Green G, Fox JJ, Lupold SE, Mease RC, Pomper MG. Sequential SPECT and optical imaging of experimental models of prostate cancer with a dual modality inhibitor of the prostate-specific membrane antigen. Angew. Chem., Int. Ed. 2011; 50:9167–9170.
37. Silver DA, Pellicer I, Fair WR, Heston WD, Cordon-Cardo C. Prostate-specific membrane antigen expression in normal and malignant human tissues. Clin. Cancer Res. 1997; 3:81–85. [PubMed: 9815541]
38. de la Taille A, Cao Y, Sawczuk IS, Nozemu T, d'Agati V, McKiernan JM, Bagiella E, Buttyan R, Burchardt M, Olsson CA, Bander N, Katz AE. Detection of prostate-specific membrane antigen expressing cells in blood obtained from renal cancer patients: a potential biomarker of vascular invasion. Cancer Detect. Prev. 2000; 24:579–588. [PubMed: 11198272]
39. Kinoshita Y, Kuratsukuri K, Landas S, Imaida K, Rovito PM Jr, Wang CY, Haas GP. Expression of prostate-specific membrane antigen in normal and malignant human tissues. World J. Surg. 2006; 30:628–636. [PubMed: 16555021]
40. Mesters JR, Barinka C, Li W, Tsukamoto T, Majer P, Slusher BS, Konvalinka J, Hilgenfeld R. Structure of glutamate carboxypeptidase II, a drug target in neuronal damage and prostate cancer. Embo J. 2006; 25:1375–1384. [PubMed: 16467855]
41. Banerjee SR, Pullambhatla M, Byun Y, Nimmagadda S, Green G, Fox JJ, Horti A, Mease RC, Pomper MG. 68Ga-labeled inhibitors of prostate-specific membrane antigen (PSMA) for imaging prostate cancer. J. Med. Chem. 2010; 53:5333–5341. [PubMed: 20568777]
42. Liu T, Wu LY, Kazak M, Berkman CE. Cell-Surface labeling and internalization by a fluorescent inhibitor of prostate-specific membrane antigen. Prostate. 2008; 68:955–964. [PubMed: 18361407]
43. Kularatne SA, Venkatesh C, Santhapuram HK, Wang K, Vaitilingam B, Henne WA, Low PS. Synthesis and biological analysis of prostate-specific membrane antigen-targeted anticancer prodrugs. J. Med. Chem. 2010; 53:7767–7777. [PubMed: 20936874]
44. Humblet V, Misra P, Bhushan KR, Nasr K, Ko YS, Tsukamoto T, Pannier N, Frangioni JV, Maison W. Multivalent scaffolds for affinity maturation of small molecule cell surface binders and their application to prostate tumor targeting. J. Med. Chem. 2009; 52:544–550. [PubMed: 19108655]

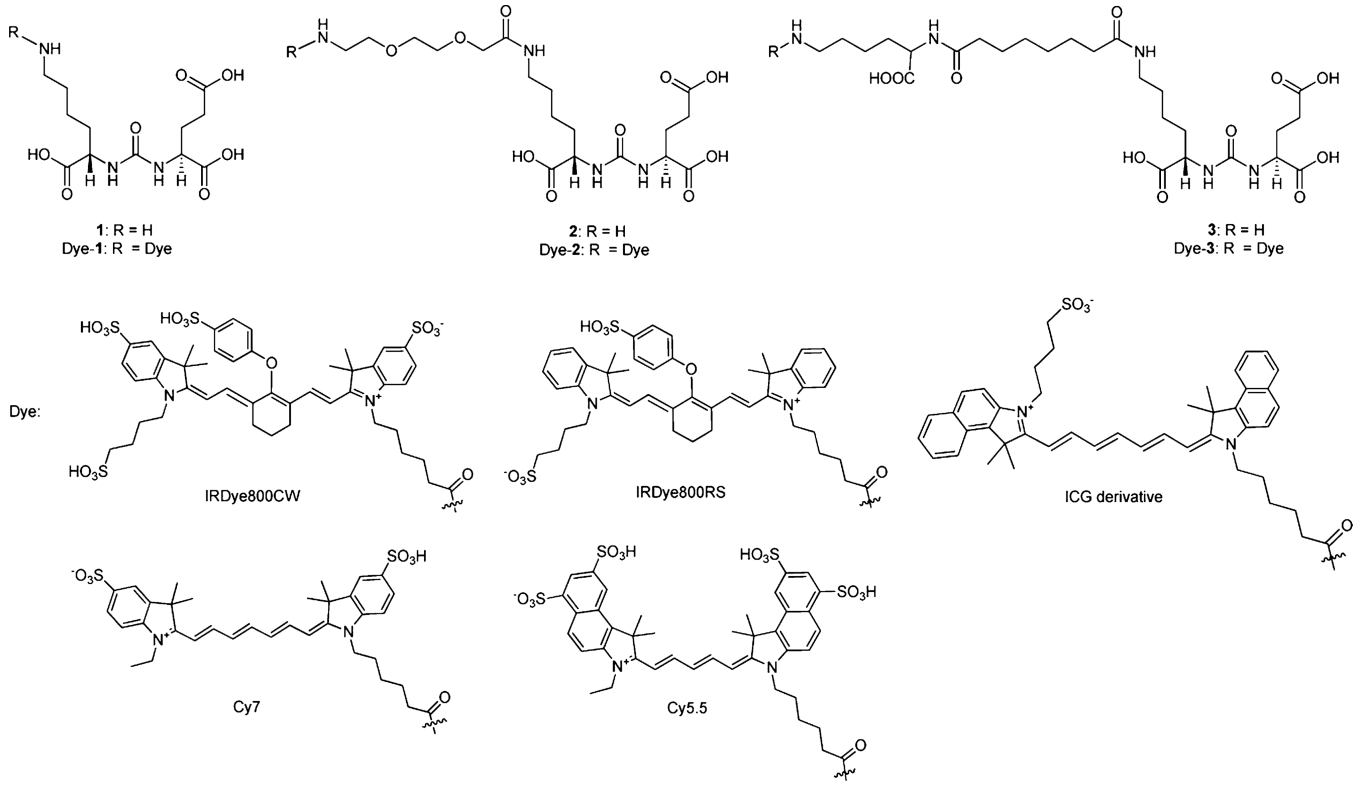

Figure 1.
Structures of PSMA-based near-infrared fluorescent imaging agents.

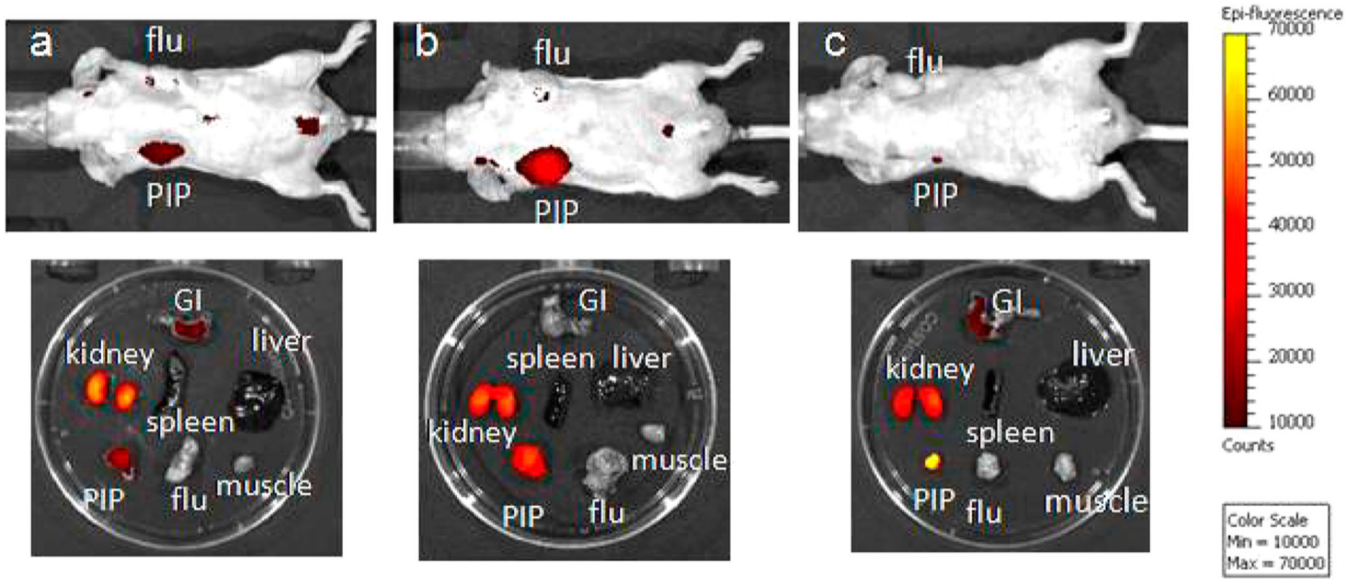

Figure 2.

Whole body and ex vivo organ imaging of mice with PSMA+ PC3 PIP and PSMA- PC3 flu tumors at 24 h postinjection of 1 nmol of (a) Cy5.5-**1**, (b) Cy5.5-**2**, and (c) Cy5.5-**3**.

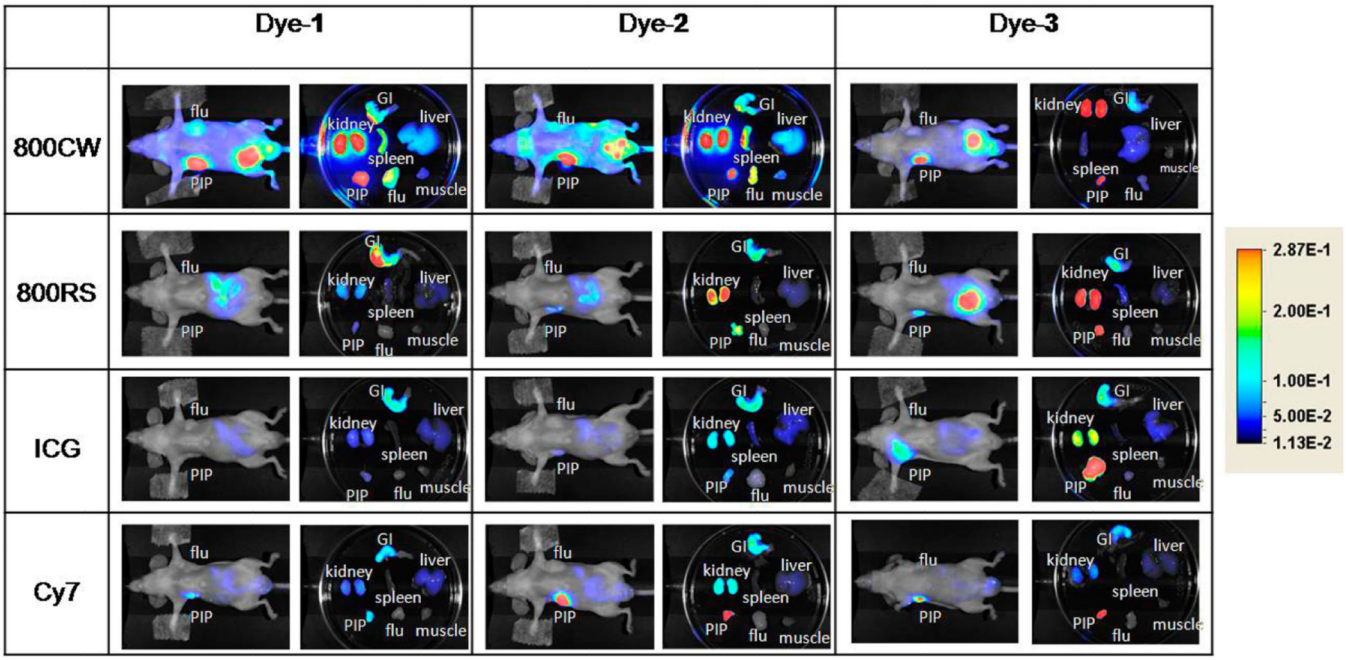

Figure 3.

Whole body and ex vivo organ imaging of mice with PSMA+ PC3 PIP and PSMA- PC3 flu tumors at 24 h postinjection of 1 nmol of the indicated dye–urea conjugates.

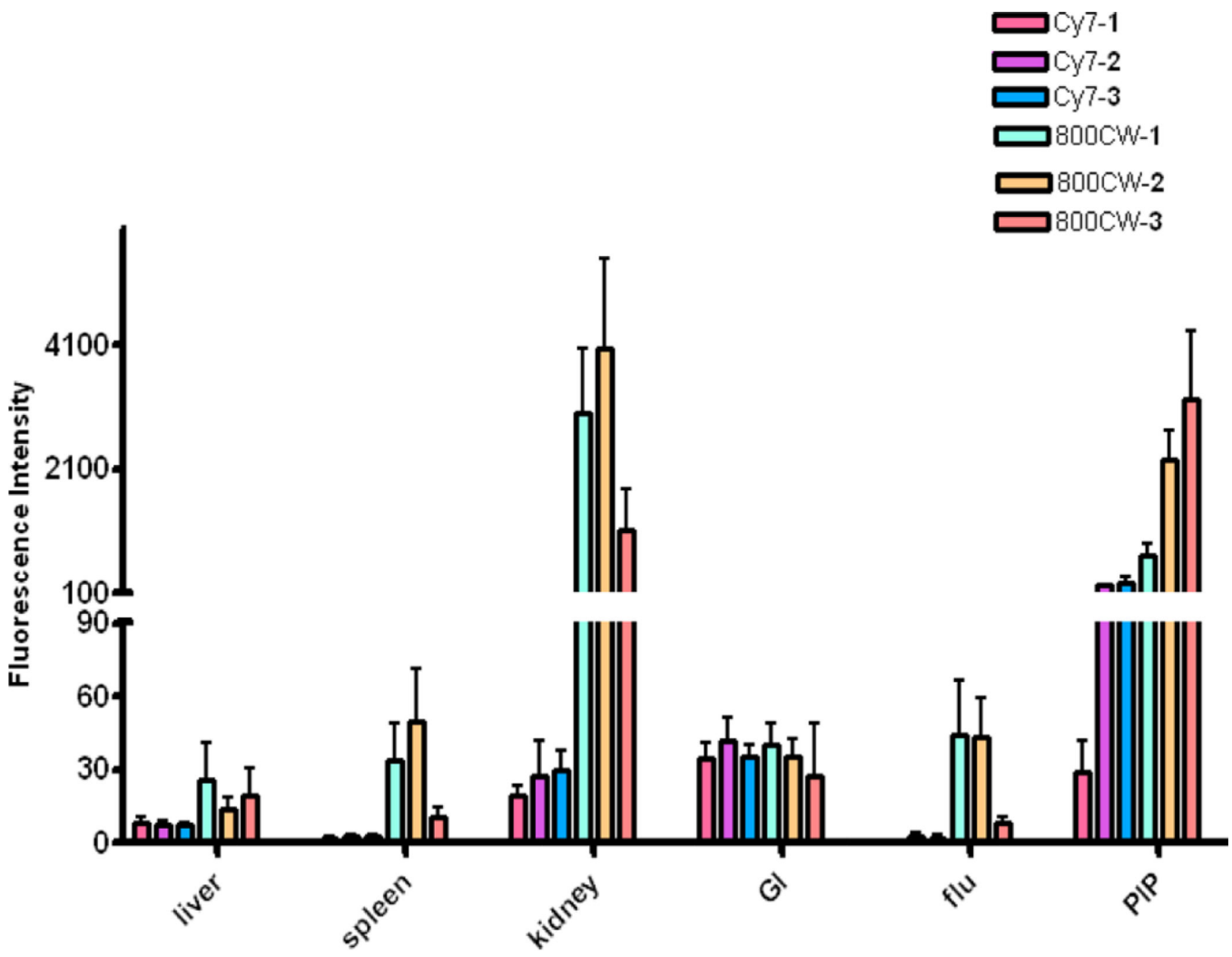

Figure 4.

Biodistribution data at 24 h postinjection from regions of interest (ROI) drawn over organs displayed in ex vivo images and normalized to muscle. Four animals were imaged per agent. Values are represented as mean ± SEM.

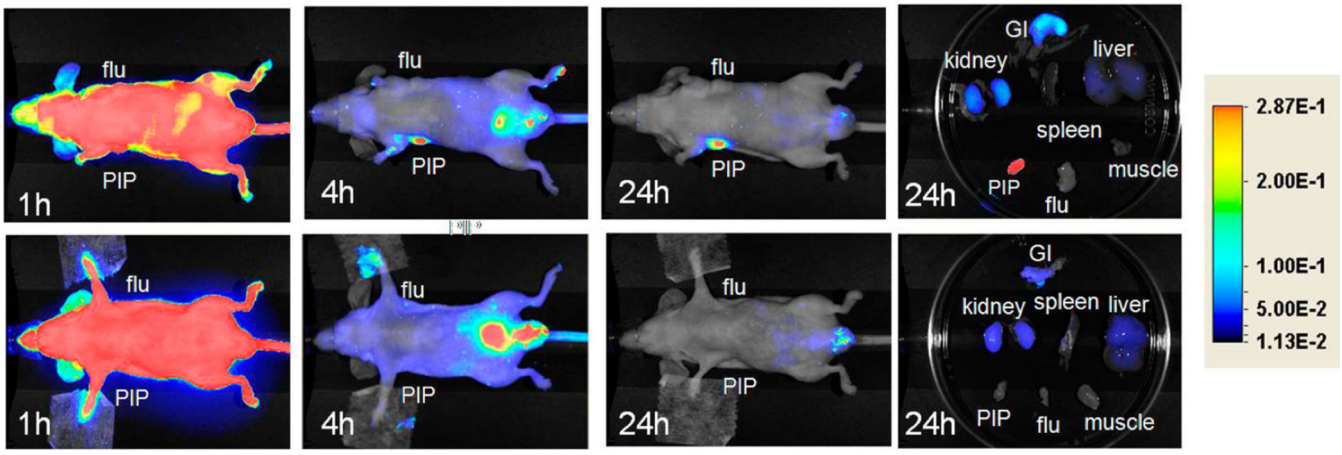

Figure 5.

Top row: Images after administration of 1 nmol Cy7-**3** at (left to right) 1, 4, and 24 h postinjection, as well as images of the excised organs at 24 h postinjection. Bottom row: Image after administration of 1 nmol Cy7-**3** + 1 mmol DCIBzL, a high-affinity ligand for PSMA (blocker) at same time points as above. Note lack of uptake in the mice treated with DCIBzL, indicating binding specificity.

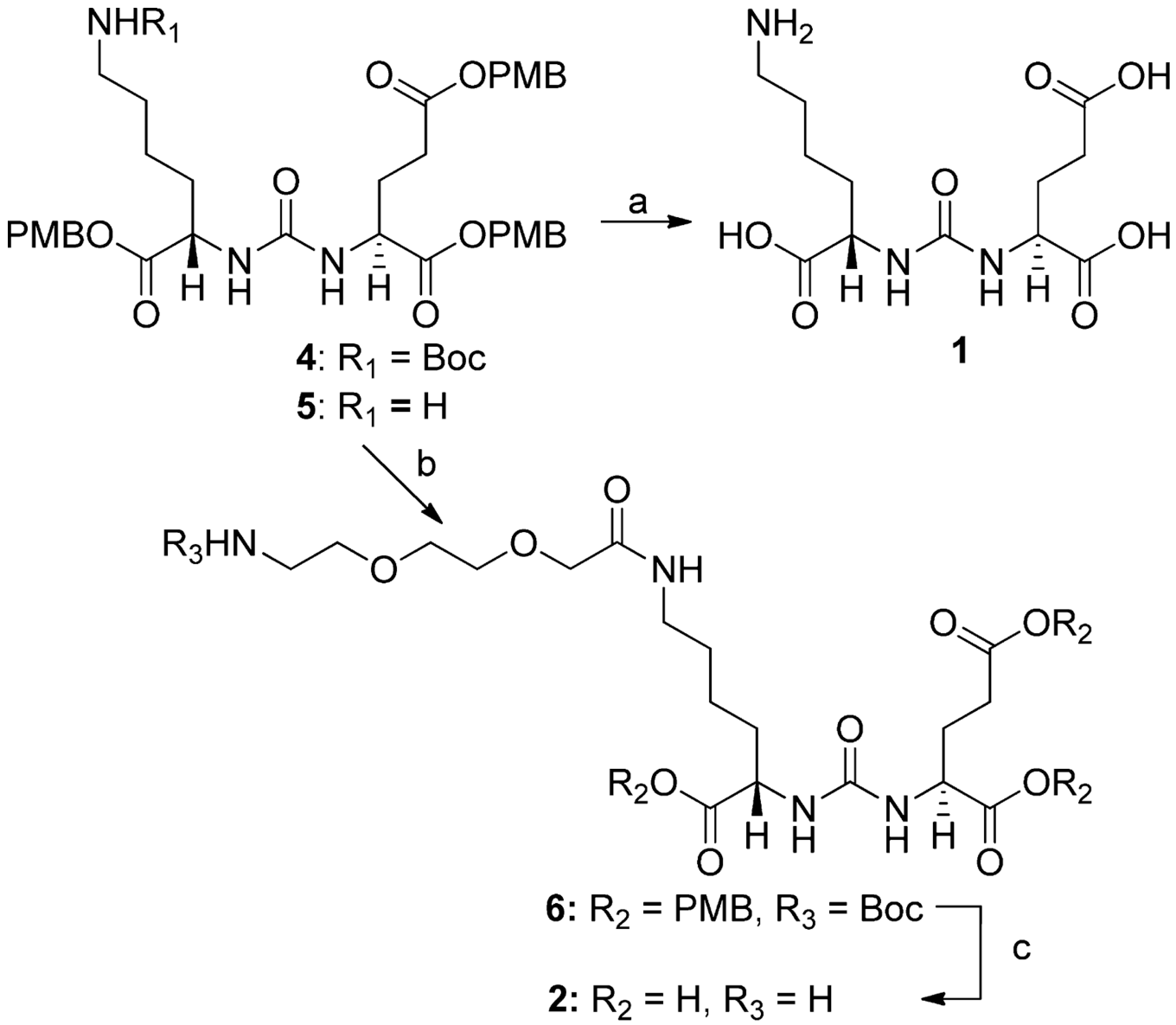

Scheme 1[a]

[a](a) TFA/anisole; (b) Boc-NH($CH_2CH_2O)_2CH_2COOH$, TBTU, *N*,*N*-diisopropylethylamine; (c) TFA/anisole.

Table 1

PSMA in Vitro Inhibitory Activities[a]

compound	K_i (pM)
800CW-**1**	70 ± 5[b]
800CW-**2**	40 ± 10[b]
800CW-**3**	20 ± 5[b]
800RS-**1**	100 ± 10[cd]
800RS-**2**	200 ± 50[b]
800RS-**3**	4 ± 0.5[c]
ICG-**1**	700 ± 10[cd]
ICG-**2**	400 ± 60[cd]
ICG-**3**	200 ± 5[cd]
Cy7-**1**	1 ± 0.5[c]
Cy7-**2**	7 ± 0.4[b]
Cy7-**3**	5 ± 0.2[c]
Cy5.5-**1**	90 ± 40[b]
Cy5.5-**2**	50 ± 20[b]
Cy5.5-**3**	50 ± 2[c]

[a] Values are in K_i ± SEM.

[b] $n = 4$.

[c] $n = 2$.

[d] Measured in DMSO; all others in water.